

## INFLUENCE OF TEMPERATURE AND EXPLOITATION TIME ON FATIGUE STRENGTH AND MICROSTRUCTURE OF WELDED JOINTS OF A-387Gr.B STEEL

I. ČAMAGIĆ<sup>1</sup>, S. JOVIĆ<sup>1</sup>, S. MAKRAGIĆ<sup>1</sup>, P. ŽIVKOVIĆ<sup>1</sup>, Z. BURZIĆ<sup>2</sup>

<sup>1</sup> University of Pristina, Faculty of Technical Sciences, Kosovska Mitrovica, Serbia;

<sup>2</sup> Military Technical Institute, Belgrade, Serbia

The main goal of the paper was to analyze the influence of temperature and exploitation time on fracture resistance of welded joint constituents of a new and exploited low-alloyed A-387Gr.B steel (Cr–Mo type) under action of dynamic load and change of mechanical properties. The exploited parent metal, as a part of a reactor mantle, is in the damage repair stage, i.e. a part of its mantle is being replaced with a new material. Wohler's curves were constructed, i.e. fatigue strength as material resistance to crack initiation was determined at the room and working temperature, testing of welded joint and microstructural analysis of parent metal, weld metal and heat affected zones was carried out. Based on the testing results, analysis of the fracture resistance as well as the microstructural changes represent the comparison of values obtained for characteristic areas of the welded joint and the justification of the selected welding technology.

**Keywords:** *crack, low-alloyed steels, welded joints, fatigue strength, mechanical properties.*

Проаналізовано вплив температури і часу експлуатації на опір руйнуванню компонентів зварних з'єднань неексплуатованої та експлуатованої низьколегованої сталі марки А-387Gr.B (типу Cr–Mo) за дії динамічного навантаження і зміни механічних властивостей. Частина експлуатованого металу оболонки реактора замінено новим матеріалом. Побудовано криві Велера: визначено опір матеріалу зародженню тріщини за кімнатної і робочої температур; виконано випробування зварного з'єднання і мікроструктурний аналіз вихідного металу зварного шва і зон термічного впливу. Порівняно опір руйнуванню, а також визначено мікроструктурні зміни характерних ділянок зварного з'єднання, і обґрунтовано обрану технологію зварювання.

**Ключові слова:** *тріщина, низьколеговані сталі, зварні з'єднання, втомна міцність, механічні властивості.*

**Introduction.** A long-time exploitation period of a pressure vessel – reactor (over 40 years) caused a certain damage to the reactor mantle. The occurrence of this damage demanded a thorough inspection of the reactor structure itself, along with repairing of damaged parts. Reactor repairs included replacing of a part of the reactor mantle with new material. The pressure vessel considered here was made of low-alloy Cr–Mo A-387Gr.B steel in accordance with ASTM standard with 0.8...1.15% Cr and 0.45...0.6% Mo. For the designed work parameters ( $p = 35$  bar and  $t = 537^\circ\text{C}$ ) the material is in the area where it is prone to decarbonization of the surface in contact with hydrogen. As a consequence of surface decarbonization, material strength may be reduced. The reactor represents a vertical pressure vessel with a cylindrical mantle. Deep lids are welded on the top and bottom sides of the mantle of the same quality as the mantle itself. Inside the reactor the most important process in the motor gasoline production stage takes place and it involves platforming in order to change the hydrocarbon compounds structure and thus achieving a higher-octane rating. Testing of the new and exploited parent metal

(PM) as well as the welded joint components (weld metal (WM) and heat affected zones (HAZ)), low-alloyed steel from which reactor is made, was performed.

The exploited PM was made of A-387Gr.B steel with a thickness of 102 mm. Chemical composition and mechanical properties (Table 1) of the exploited and new PM according to the test documentation are given below. Chemical composition of the exploited and new PM specimens (mass%) is as follows: specimen E (C – 0.15, Si – 0.31, Mn – 0.56, P – 0.007, S – 0.006, Cr – 0.89, Mo – 0.47, Cu – 0.027); specimen N (C – 0.13, Si – 0.23, Mn – 0.46, P – 0.009, S – 0.006, Cr – 0.85, Mo – 0.51, Cu – 0.035).

**Table 1. Mechanical properties of the exploited and new PM specimens**

Specimen designation	Yield stress, $R_{p0.2}$	Tensile strength, $R_m$	Elongation, A, %	Impact energy, J
	MPa			
E	320	450	34.0	155
N	325	495	35.0	165

Welding of steel sheets made of the exploited and new PM was performed in two stages, according to the requirements given in the welding procedure provided by a welding specialist, and these stages include: root weld of specimen E, using a coated LINCOLN S1 19G electrode (AWS: E8018-B2), and filling by arc welding under powder protection, where wire denoted as LINCOLN LNS 150 and powder denoted as LINCOLN P230 were used as additional materials.

Chemical composition of the coated electrode LINCOLN S1 19G and the wire LINCOLN LNS 150 according to the test documentation are given below. Chemical composition of additional welding materials is as follows: LINCOLN S1 19G: C – 0.07, Si – 0.31, Mn – 0.62, P – 0.009, S – 0.010, Cr – 1.17, Mo – 0.54; LINCOLN LNS 150: C – 0.10, Si – 0.14, Mn – 0.71, P – 0.010, S – 0.010, Cr – 1.12, Mo – 0.48. Their mechanical properties, also according to the test documentation are given in Table 2.

**Table 2. Mechanical properties of additional materials**

Additional material	Yield stress, $R_{p0.2}$	Tensile strength, $R_m$	Elongation, A, %	Impact energy, J at 20°C
	MPa			
LINCOLN S1 19G	515	610	20	> 60
LINCOLN LNS 150	495	605	21	> 80

A butt welded joint was made with a U-weld. The shape of the groove for welding preparation was chosen based on the sheet thickness, in accordance with appropriate standards SRPS EN ISO 9692-1:2012 [2] and SRPS EN ISO 9692-2:2008 [3].

**Determining of fatigue strength.** Metal fatigue is defined as the process of cumulative damage under the effect of variable load which is manifested in the occurrence of cracks and fracture. Fatigue strength of welded joints is determined from testing of the specimen with variable load that leads to initiation of cracks or fracture. In case of reactors, i.e. pressure vessels which operate under increased pressure and temperature conditions, high-cycle fatigue tests are of particular importance. Strength of a welded joint under variable loads, that occur in non-stationary reactor work modes during starting and stopping, is an important characteristic for assessing the integrity and remaining life. At the same time, it should be taken into account that a crack-like damage occurs after a large number of changes in the load at stresses much lower than

the yield stress (high-cycle fatigue). At load levels lower than yield stress, typical of high-cycle fatigue, it is a common practice to perform a test in rigid mode.

High-cycle fatigue depends on the properties of the welded joint constituents. The characteristics of high-cycle fatigue start changing significantly only at temperatures above 400°C for steel used for pressure vessels and their welded joints.

Testing of the effects of temperature and exploitation duration on the behavior of the new PM as well as on the butt welded joint subjected to variable load was performed to determine the points in the S–N-diagram (drawing of the Wohler’s curve) and fatigue strength ( $S_f$ ) welding procedure, as well as specimens testing were carried out according to standards ASTM E466, ASTM E467 and ASTM E468 [4–6]. The shape of the specimen tested under variable load is shown in Fig. 1.

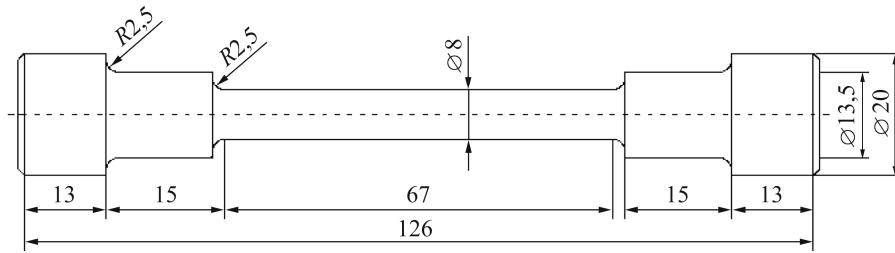


Fig. 1. Specimen for dynamic tests according to ASTM E466.

Testing was performed on a high frequency pulsator. The values of the achieved frequency ranged between 115 and 165 Hz, depending on the load and testing temperature. In order to fully evaluate the behavior of materials subjected to variable load, while taking into account the dimension of the specimen, the most critical case of variable load was considered with the use of variable load that alternated between tension and pressure ( $R = -1$ ).

During this testing, it is a general rule to determine only the number of load changes until fracture under the load with a constant range, and the standard requires only data about the stress magnitude at which crack initiation and fracture after a specific number of cycles does not occur (typically between  $10^6$  and  $10^8$  cycles). For steel materials, standard ASTM E466 defines  $S_{\text{stress}}$ ,  $S_f$  after  $10^7$  cycles.

The effect of exploitation duration and temperature on  $S_{\text{stress}}$ ,  $S_f$ , i.e. maximum dynamic stress at which there is no initiation of crack-like defects in smooth structure shapes, is graphically shown in the form of Wohler’s curves (S–N-diagrams) in Fig. 2a for a butt welded joint specimens and in Fig. 2b for specimens cut out from the new PM [1].

Testing of specimens of the PM was not performed, since all welded joint specimens cracked in the zone of the exploited PM, hence these tests provided the characteristics of the welded joint and PM.

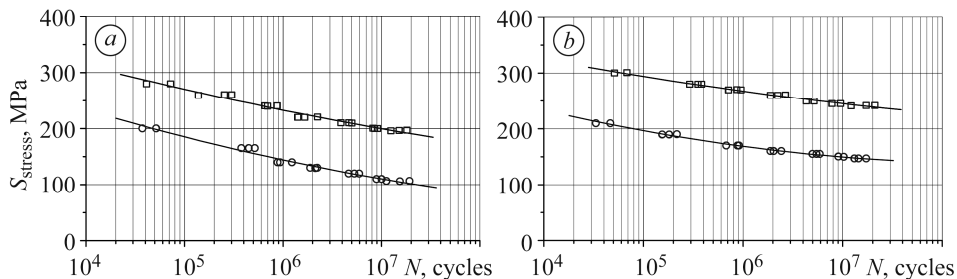


Fig. 2. S–N-diagram for specimens cut out from the butt welded joint (a) and from the new PM (b) and tested at room and working temperature:  $\square$  – 20°C;  $\circ$  – 540°C.

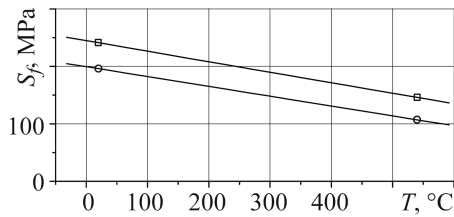


Fig. 3. Change of  $S_f$  values for specimens cut out from the new PM and a butt welded joint depending on the temperature: □ – new PM; ○ – welded joint.

In order to draw a Wohler's curve and to determine the fatigue strength, it is necessary to test the specimens at 6 to 7 different levels of load. According to standard ASTM E 466 for every load level, three specimens were tested, which made a total of 21 specimens. Due to this, such tests are very expensive and are only justified when data for designing are necessary, first of all from the aspect of fatigue and fracture mechanics, in other words when parts subjected to long-term variable loads are designed as a part of the total designed structure life.

The effect of testing temperature on  $S_{\text{stress}}$ ,  $S_f$  obtained by testing of specimens cut out from a butt welded joint and the new PM is shown in Fig. 3 [1].

**Macro and microstructural testing.** For a successful application of A-387Gr.B steel and to obtain its maximal creep resistance, guaranteed mechanical properties are requested at higher temperatures, as well as creep resistance at exploitation temperatures in a period that can be longer than 150000 h. These properties are obtained with the proper thermal treatment, providing the structure consisting of ferrite and bainite. Very fine carbides, which start to sediment during this thermal treatment, segregate at the grain border, as well as within the grain which can be seen under high magnification [7, 8].



Fig. 4. Welded joint macrorecording.

Carbide precipitation, which begins during thermal treatment for residual stress elimination, continues during exploitation at exploitation temperatures and pressures [9, 14]. Appearance of these brittle phases can be ascertained by metallographic analysis under high magnification. This testing was conducted in order to evaluate the exploitation period of the parent metal and the welded joint components in respect of microstructural properties change. Macrorecording of a butt welded joint of the new PM and exploited PM is given in Fig. 4 [1].

After the butt welded joint etching we can clearly differentiate the new and exploited parent metal; heat affected zone from the both sides; weld metal with well-marked groove filling zone.

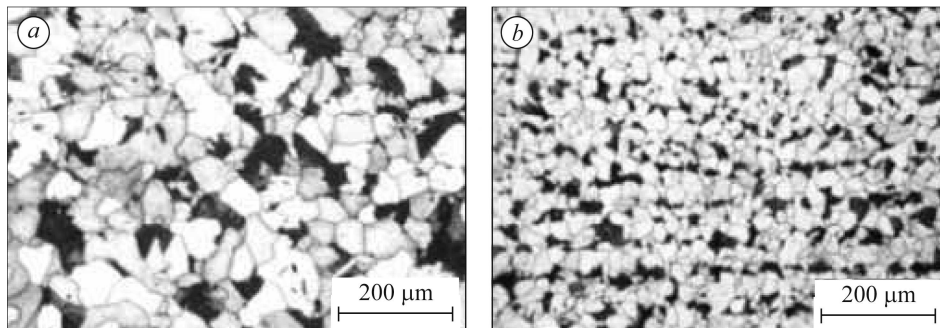


Fig. 5. Microstructure of the exploited PM (a) and new PM (b), ferrite-perlite structure.

Both parent metals show even structure, which consists of bright polygonal ferrite crystals and transformed areas that can be analyzed under high magnification. These

transformed areas represent dark surfaces of perlite that looks like a compact dark microconstituent. Microstructure of the PM that was in exploitation for over 40 years is shown in Fig. 4 and the PM microstructure is shown in Fig. 5 [1]. Difference is in a grain size. A newly installed parent metal has a structure with a grain size 5 according to ASTM scale, while the exploited material has a structure with a grain size 3 according ASTM scale.

It is clear that at  $\times 100$  magnification it is impossible to notice essential difference between the used and a new material, except in the grain size.

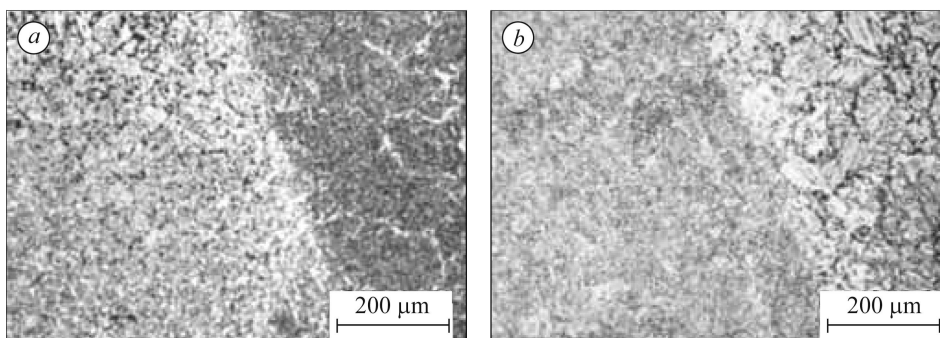


Fig. 6. HAZ microstructure on the used (a) and new PM (b).

Microstructure in the HAZ on the exploited and new PM side is shown in Fig 6 [1]. It consists of ferrite, bainite and perlite. A bainite in the HAZ is formed as a consequence of higher cooling rate of a part of the parent metal that was heated to the austenitizing temperature during welding. A bainite level reduces increase of the distance from the joint line.

A weld metal structure with large dendrite created as a consequence of the foundry bath size and dimensions of the welded plates is shown in Fig. 7 [1].

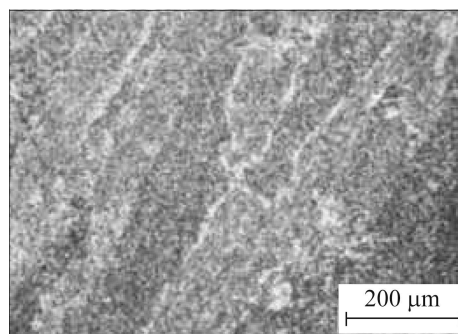


Fig. 7. WM microstructure, dendrite structure of the weld metal.

Higher magnification ( $\times 500$  and more), enabled revealing differences in structural properties of the exploited and new PM. Exploitation period of more than 40 years affected the presence of carbide on the grain borders and within a grain. The carbides amount in the new PM is significantly less and the carbides are smaller (Fig. 8) [1].

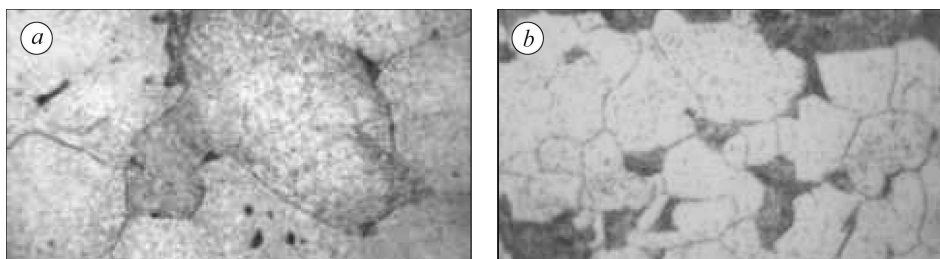


Fig. 8. Used PM (a) and new PM (b) microstructure.

## CONCLUSIONS

The material resistance to crack initiation is determined by fatigue strength testing of materials. It is the maximum value of stress at which crack initiation on smooth specimens does not occur. The higher the ratio of fatigue strength to yield stress, the better

its resistance to crack initiation is. By analyzing the results obtained by high-cycle fatigue testing of smooth specimens for the purpose of drawing the Wohler's curves and determining fatigue strength, it can be seen that exploitation and duration have a dominant effect on the obtained values of fatigue strength. In case of testing of the welded joint specimens made of the exploited PM at room temperature, the ratio of fatigue strength to yield stress is 0.68, i.e. the obtained value of fatigue strength represents 68% of the yield stress. All welded joint specimens broken, while being tested with loads higher than the fatigue load, were cracked either in the exploited PM or HAZ on the side of the exploited PM. The effect of testing temperature is such that an increase in temperature leads to the reduced fatigue strength. In this case, the welded joint specimens were cracked either in the exploited PM or in its HAZ. Crack initiation resistance for tests at 540°C decreases, i.e. the tendency towards brittle fracture increases. Test results and their analysis have justified the choice of the welding technology for the purpose of replacing the part of the reactor mantle.

**Acknowledgements.** *Parts of this research were supported by the Ministry of Sciences and Technology of Republic of Serbia through Mathematical Institute SANU Belgrade Grant OI 174001 "Dynamics of hybrid systems with complex structures". Faculty of Technical Sciences University of Pristina in Kosovska Mitrovica.*

1. Čamagić I. Investigation of the effects of exploitation conditions on the structural life and integrity assessment of pressure vessels for high temperatures (Doctoral dissertation, doctoral thesis, University of Pristina // Faculty of Technical Sciences with the seat in Kosovska Mitrovica. – 2013.
2. ISO 9692-1:2003. Welding and allied processes – Recommendations for joint preparation – Part 1: Manual metal-arc welding, gas-shielded metal-arc welding, gas welding, TIG welding and beam welding of steels. – 2003.
3. EN ISO 9692-2:1998. Welding and allied processes – Joint preparation – Part 2: Submerged arc welding of steels. – 1998.
4. ASTM E466-07. Standard practice for conducting force controlled constant amplitude axial fatigue tests of metallic materials // ASTM Int. – West Conshohocken, PA, 2007.
5. ASTM E467-89. Standard Practice for Verification of Constant Amplitude Dynamic Loads in an Axial Load Fatigue Testing Machine // Annual Book of ASTM Standards. – 1989. – Vol. 03.01. – P. 577.
6. ASTM E468-89. Standard Practice for Presentation of Constant Amplitude Fatigue Test Results for Metallic Materials // Annual Book of ASTM Standards. – 1989. – Vol. 03.01. – P. 582.
7. Kikuta Y. Classification of microstructures in low-C, low-alloy steel weld metal and terminology // Committee of Welding Metallurgy of the Japan Welding Society (p. 15). Report No. IX-1281-83. – 1983.
8. Metals Handbook. Vol. 6: Metallography // ASM Int. – 1998. – P. 1124.
9. Cochrane R. C. Weld Metal Microstructures: A State-of-the Art review. – International Institute of Welding, 1982. – 25 p.
10. Kasatkin B. S., Kozlovets O. N. Microstructure and low-alloy steel welded joints properties (Review) // Paton Welding Journal C/C of Avtomaticheskaja Svarka. – 1989. – № 7. – P. 1–11.
11. Burzić Z., Čamagić I., and Sedmak A. Fatigue strength of a low-alloyed steel welded joints // The 3<sup>rd</sup> IIW South–East European Welding Congress, "Welding and Joining Technologies for a Sustainable Development and Environment", June 3–5, 2015. – Romania: Timisoara, 2015. Proc. (P. 135–138). ISBN 978-606-554-955-5.
12. Influence of temperature and exploitation time on tensile properties and microstructure of specific welded joint zones / I. Čamagić, N. Vasić, S. Jović, Z. Burzić, and A. Sedmak // 5<sup>th</sup> Int. Congress of Serbian Society of Mechanics Arandjelovac, Serbia. – 2015, June.
13. Балицький О. І., Костюк І. Ф. Міцність зварних з'єднань Cr–Mn сталей з підвищеною концентрацією азоту у водневовмісних середовищах // Фіз.-хім. механіка матеріалів. – 2009. – № 1. – P. 88–96.  
(Balys'kyi O. I. and Kostyuk I. F. Strength of welded joints of Cr–Mn steels with elevated content of nitrogen in hydrogen-containing media // Materials Science. – 2009. – № 1. – P. 97–107.)
14. Balitsky A. I., Kostyuk I. F., and Krokhmalny O. A. Physical-mechanical non-homogeneity of welded joints of high-nitrogen Cr Mn steels and their corrosion resistance // Paton Welding Journal C/C of Avtomaticheskaja Svarka. – 2003. – № 2. – P. 26–29.

Received 06.04.2017